Non-stick Polymer Coatings for Energy-based Surgical Devices Employed in Vessel Sealing

Sung Kil Kang,[a] Paul Y. Kim,[a] Il Gyo Koo, Ho Young Kim, Jae-Chul Jung, Myeong Yeol Choi, Jae Koo Lee, George J. Collins*

Energy-based surgical devices are widely used to fuse tissues and seal vessels, but tissue adhesion to the instrument complicates the procedure. We deposit a robust non-stick coating on the jaws of LigaSure™ tissue fusion devices by employing an atmospheric pressure RF-driven plasma with hexamethyldisiloxane (HMDSO) entrained in argon carrier gas. The hydrophobicity, surface energy, surface topography, and chemical characteristics of deposited films are characterized by water contact angle measurements, surface energy test pens, atomic force microscopy, and Fourier transform infrared spectroscopy, respectively. We demonstrate significantly reduced tissue adhesion to HMDSO polymer film-coated instruments during the tissue fusion procedure in comparison with uncoated and chromium nitride-coated instruments.

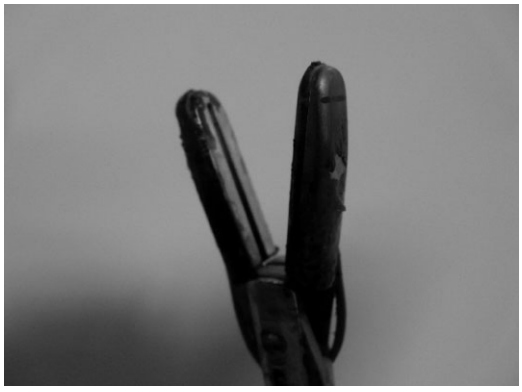

1. Introduction

Hydrophobic surface modifications have attracted interest in various applications including self-cleaning surfaces,[1,2] corrosion protection,[3,4] waterproof textiles,[5] and medical devices.[6] The medical industry continues to require advancements in biocompatible coatings and surface treatment processes with specific electrical properties and surface functionalization. Polymer coatings that impart antimicrobial, antithrombogenic, lubricious, or non-stick properties have generated intense interest.[7,8] A number of technologies are available for depositing polymer coatings onto a surface.

Conventional wet chemical polymerization requires both long-reaction times at elevated temperatures and the use of catalysts. Plasma-assisted deposition of polymeric coatings is a rapid, low-temperature method that avoids the use of environmentally hazardous solvents employed in wet chemical processing. In plasma-enhanced chemical vapor deposition (PECVD), free electrons quickly break chemical bonds in the monomer precursor to generate an unstable intermediate chemical, which then polymerizes to form a stable coating. Non-atmospheric PECVD requires an expensive low-pressure vacuum chamber,[9,10] load locks, and low-throughput batch processing. Atmospheric pressure PECVD presents an advantage in that depositions can occur in open air as part of the inline manufacturing.[11–13] Moreover, atmospheric pressure PECVD occurs at low temperature so that temperature sensitive substrates may be coated without thermal damage.[14]

Atmospheric pressure PECVD of hexamethyldisiloxane (HMDSO) is used in the present study to create a physically

S. K. Kang, H. Y. Kim, J. K. Lee
Department of Electronic and Electrical Engineering, Pohang University of Science and Technology, Pohang 790-784, Republic of Korea
P. Y. Kim, I. G. Koo, J.-C. Jung, M. Y. Choi, Dr. G. J. Collins
Department of Electrical and Computer Engineering, Colorado State University, Fort Collins, CO 80523, USA
E-mail: gcollins@engr.colostate.edu

[a] These authors contributed equally to this work.

DOI: 10.1002/ppap.201100155

robust non-stick polymer coating. HMDSO is an organosilicon compound with reportedly minimal toxicity commonly employed as a precursor for SiO_x film in PECVD.[15–18] Deposition of HMDSO polymer by argon plasma was initially carried out on a glass substrate to determine the optimum conditions for coating the metallic jaws of surgical devices employed in tissue sealing.

Our specific aim was to develop a non-stick coating for LigaSure™ tissue fusion devices manufactured by Covidien (Mansfield, MA). LigaSure™ instruments are used in a range of laparoscopic and open surgical procedures to permanently fuse vessels and tissue bundles via a combination of mechanical pressure and bipolar electrical energy applied between the electrode jaws. Undesired tissue adhesion to the jaw surface during the procedure carries a risk of tearing the sealed tissue as the jaw is opened forcefully. We compare atmospheric pressure PECVD non-stick coatings to conventional vacuum-deposited non-stick coatings and report significantly reduced tissue adhesion in the atmospheric pressure PECVD coatings.

2. Experimental Section

2.1. Plasma Jet Configuration

The atmospheric pressure coaxial plasma jet is depicted in cross-section in Figure 1. It consisted of two concentric electrodes made of aluminum tubes interposed by a ceramic tube acting as a dielectric barrier. The inner electrode was powered by a 13.56 MHz power supply (Cesar-133, Advanced Energy) through a homemade L-C matching unit. Reflected power was less than 5% of forward power in all experiments. The inner electrode (outside diameter of 3.5 mm and internal diameter of 3.1 mm) and the outer-grounded electrode (height of 15 mm) terminated 3 and 2 mm, respectively, from the end of the ceramic tube (internal diameter of 6 mm).

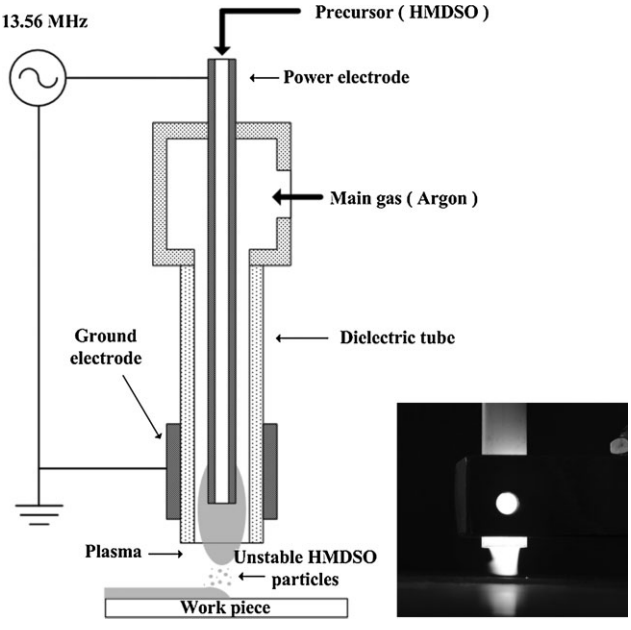

Figure 1. A coaxial plasma jet configuration employing two concentric tubes as the opposing electrodes, thereby creating an annular plasma jet.

The HMDSO monomer (Sigma–Aldrich) was aerosolized and entrained in argon carrier gas by means of a bubbler maintained at 25 °C. This entrained stream flowed through the inner electrode, which was fitted through a T-shaped PTFE housing for the introduction of main argon gas through a side port. The two gas streams were supplied separately to minimize polymer coating of the inner electrode. The concentration of entrained HMDSO monomer in the total argon gas flow was controlled from 0.1 to 3.0% (v/v) by regulating argon carrier gas flow to the bubbler. Carrier and main argon gas flows were controlled by digital flow controllers (DFC 4000, Flowtech). Main argon gas flow was fixed at 800 sccm throughout this study.

Plasma gas temperature was measured by an optical fiber thermometer (FISO-FTI-10) in contact with the end of the plasma plume. The work piece surface temperature was measured immediately following plasma deposition by an IR-thermometer (FLUKE 62).

2.2. Polymer Deposition and Characterization

Plasma deposition of HMDSO polymer was carried out on glass slides at a distance of 10 mm from the plasma jet to the substrate for 60 s. Changes in glass surface properties were determined by measuring static contact angles of sessile water droplets 2 μl in volume on the glass surface. Surface energy was measured using surface energy test pens (Arcotest) according to the manufacturer's instructions. Chemical functional group properties of the HMDSO polymer coating were analyzed by a Thermo Scientific Nicolet 6700 Fourier transform infrared spectroscopy-attenuated total reflectance (FTIR-ATR) spectrometer at various deposition conditions. Images of plasma-treated surfaces were collected using a multimode atomic force microscope (AFM) driven by a Nanoscope IIIa controller (Digital Instruments/Bruker AXS) at a scanning rate of 1 Hz in tapping mode. The mean spring constant of the tip was 42 N m^{-1} and length was 125 μm. Root-mean-square (RMS) surface roughness was calculated within a 4 μm × 4 μm scan area.

2.3. Tissue Adhesion Testing on LigaSure™ Instrument

Plasma deposition of optimized HMDSO polymer coatings was subsequently carried out on LigaSure™ Atlas instruments placed at a distance of 10 mm from the plasma jet. The instrument was serially coated at 12 different points inside and outside the jaw for 30 s at each point. This was necessary with our present point plasma geometry. HMDSO polymer-coated instruments were evaluated for the force required to open the jaws following tissue fusion of porcine uterine wall soaked in porcine blood (with heparin). Uncoated instruments and chromium nitride-coated instruments were tested for comparison. Testing was carried out over 100 sealing cycles and each data point represents the mean of ten sealing cycles.

3. Results and Discussion

3.1. Plasma Characteristics

Plasma is ignited with 10 W effective (forward-reflected) input power using a spark generator. Below 15 W input power, filamentary plasma is generated between the inner electrode and the dielectric tube. At 15 W input power, the plasma begins transition to glow discharge mode. At 25 W input power, an annular glow discharge completely fills the area around the inner electrode, forming a plume that extends 8 mm (Figure 2a and b). Although the glow plasma plume is enhanced when target material is placed at the end of the plasma, no arcing or streamer damage to the work piece is observed up to 25 W. With the addition of 1.0% HMDSO the plasma is slightly quenched and its length is reduced to 5 mm (Figure 2d). Input power higher than 25 W leads to arcing and HMDSO concentration above 2.0% results in unstable plasma.

The temperatures of the plasma gas and work piece surface are presented in Figure 3. Plasma gas temperature increases as the input power increases, reaching 107 °C with 25 W input power. With addition of 1.0% HMDSO, plasma gas temperature decreases approximately 2–5 °C. Plasma heat transfer to the work piece appears limited by the relatively short-treatment time since the surface temperature does not exceed 45 °C.

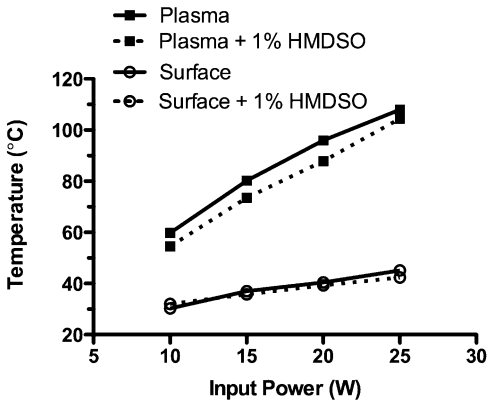

Figure 3. Plasma gas temperature (closed squares) and treated surface temperature (open circles) as a function of input power, with 1.0% HMDSO (dotted lines) and without HMDSO (solid lines). Main argon flow is fixed at 800 sccm and deposition is carried out for 60 s.

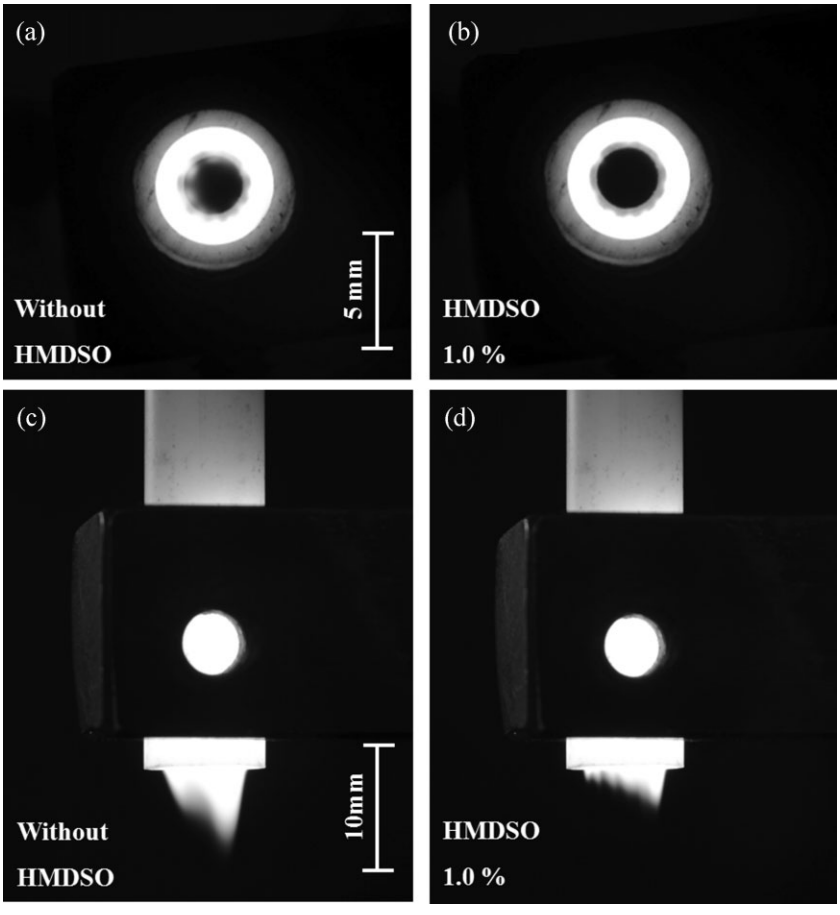

Figure 2. End-view (upper panels) and side view (lower panels) of plasma formation at 25 W input power with 1.0% HMDSO (right panels) and without HMDSO (left panels).

3.2. Surface Contact Angle

We conduct two single variable experiments to identify the input power and HMDSO concentration resulting in the greatest degree of surface hydrophobicity as determined by water contact angle measurements (Figure 4). First, with HMDSO concentration fixed at 0.5%, we observe increasing contact angle with increasing input power in the range of 10–25 W with maximum contact angle of 95.8° at 25 W (Figure 4a). Next, with input power fixed at 25 W, we observe the greatest degree of hydrophobicity at 1.0% HMDSO (Figure 4b). Overall, the maximum contact angle is 112.3° at 1.0% HMDSO and 25 W input power and the studies below are carried out under these conditions.

3.3. Surface Energy

Surface energy measured using a set of surface energy test pens is presented in Figure 5. The test pens contain fluids of defined surface tension from 32 to

DOI: 10.1002/ppap.201100155

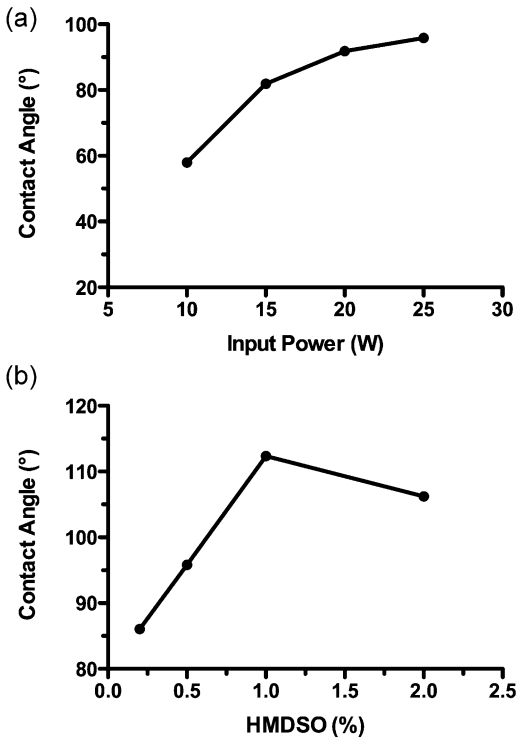

Figure 4. Static contact angles of sessile water droplets as a function of (a) input power at 0.5% entrained HMDSO monomer concentration and (b) entrained HMDSO monomer concentration at 25 W input power. Main argon flow is fixed at 800 sccm and deposition is carried out for 60 s.

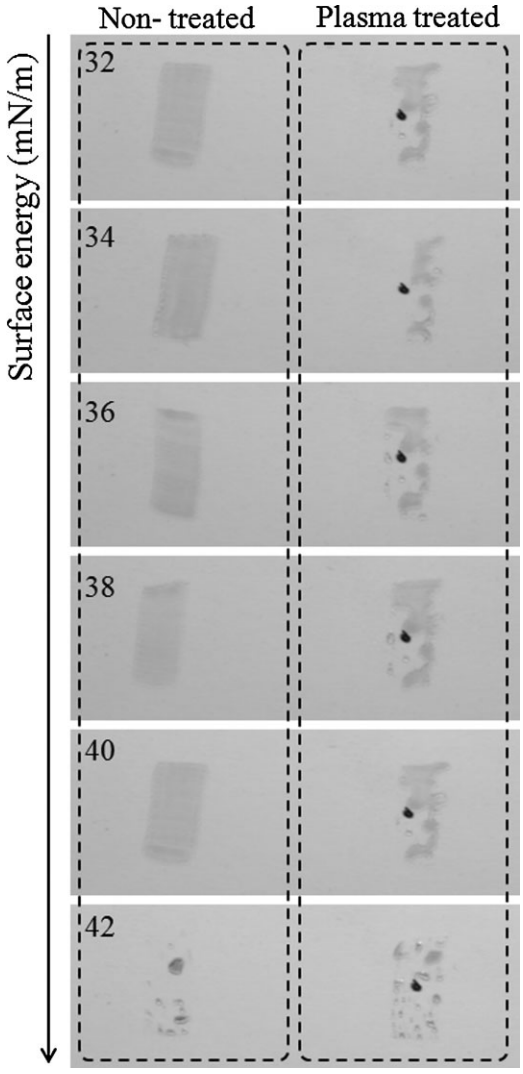

Figure 5. Surface energy measurement of non-treated (left panel) and plasma-treated (right panel) glass slides by surface energy test pens. Main argon flow is fixed at 800 sccm and deposition is carried out for 60 s at 25 W input power and 1.0% HMDSO. Surface energy is presented on the left side.

42 mN m^{-1}. If a stroke of fluid applied with the felt tip remains unchanged on the material's surface without beading, the surface energy of the material is the same or higher than the surface tension of that test pen. In the case of untreated glass slides, the test fluid does not form drops until 42 mN m^{-1}. In comparison, all of the test fluids are found to form drops on plasma-treated glass slides indicating an HMDSO polymer surface energy of approximately 32 mN m^{-1} or less. The hydrophilicity or hydrophobicity of a material is closely related to the surface energy.[19] Generally, hydrophobic surfaces have low-surface energy and these results agree well with our water contact angle measurements.

3.4. Surface Chemistry

The chemical structure of the HMDSO polymer coating deposited under 10–20 W input power and 0.2–2.0% HMDSO concentration is characterized by means of FTIR spectroscopy (Figure 6). Several bands in the 700–3 000 cm^{-1} region can be recognized. We assign these as follows: 780–800 cm^{-1} to Si–C stretching and CH_3 rocking in Si–$(CH_3)_{1-3}$, 843 cm^{-1} to Si–C stretching and CH_3 rocking in Si–$(CH_3)_3$, 900–950 cm^{-1} to Si–OH stretching, 1 000–1 100 cm^{-1} to Si–O–Si stretching, 1 273 cm^{-1} to CH_3 bending in Si–CH_3, and 2 968 cm^{-1} to CH_3 stretching.[20] The band at 2 350 cm^{-1} is attributed to carbon dioxide. As input power increases the intensity of the main Si–O–Si peak increases indicating a thicker film (Figure 6a). The chemical structure does not change significantly with variation in HMDSO concentration (Figure 6b). Film thickness increases with increasing HMDSO concentration from 0.2 to 1.0% but then decreases at 2.0%. In a previous study, Morent et al. have deposited HMDSO films using dielectric barrier discharge and reported higher deposition rates at 3.0 ppm HMDSO than at 4.0 ppm at a constant discharge power.[21] These results show that while deposition rate is dependent on monomer flow rate, while a

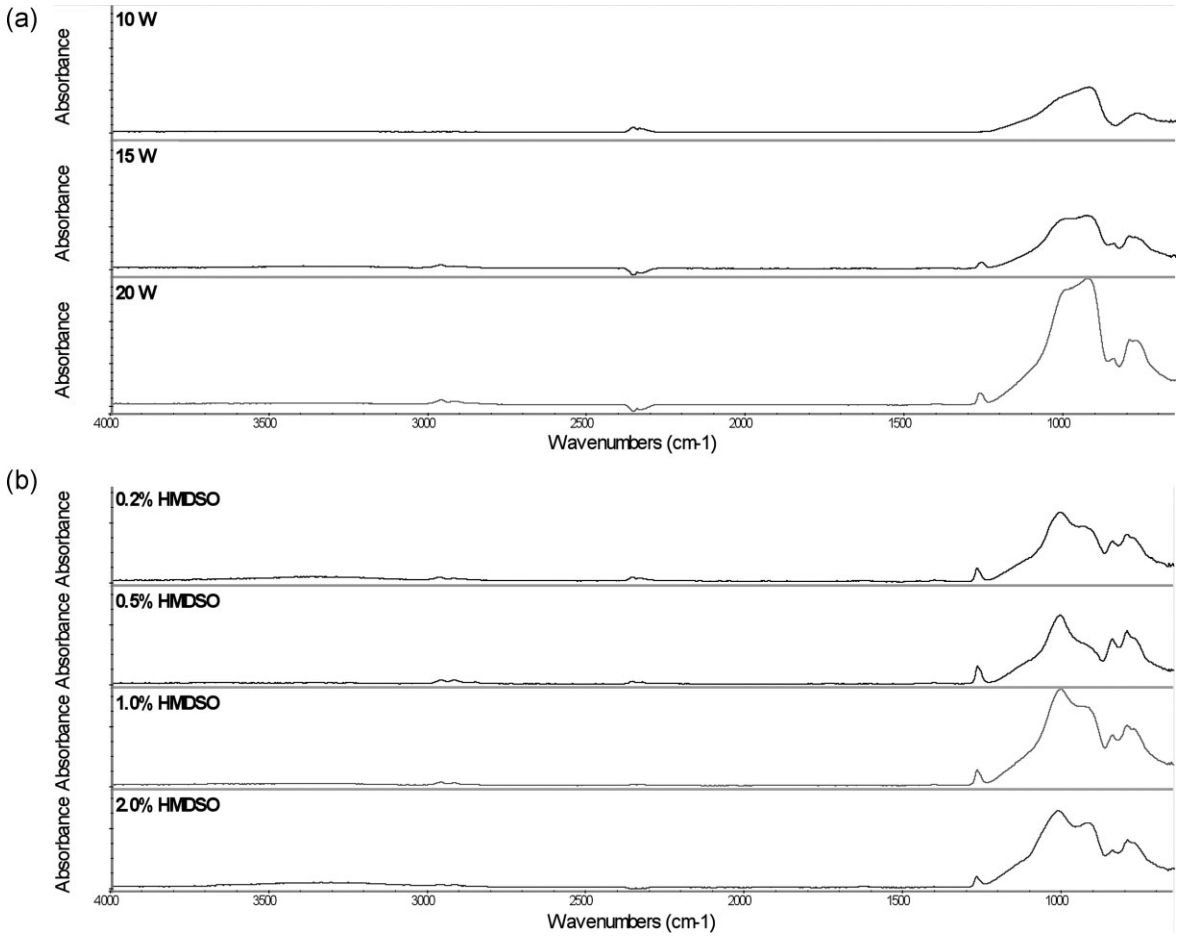

Figure 6. FTIR spectra of HMDSO polymer films deposited at (a) 10–20 W input power and 1.0% entrained HMDSO monomer concentration and (b) 0.2–2.0% entrained HMDSO monomer concentration at 25 W input power. Main argon flow is fixed at 800 sccm and deposition is carried out for 60 s.

balance of both hydrophobic (CH_3) and hydrophilic (OH) functional groups are observed in the spectra, surface modification by hydrophobic compounds appears dominant and are likely responsible for the increased hydrophobicity observed in Figure 4.

3.5. Surface Topography

Not only surface energy, but also surface topography plays an important role in determining surface properties. Synthetic hydrophobic surfaces can be fabricated by creating rough surfaces according to a relationship described by the Wenzel equation and Cassie–Baxter equation.[22,23] AFM images of non-treated and plasma-treated glass slides are presented in Figure 7. Both the non-treated and plasma-treated surfaces are relatively smooth although the RMS surface roughness increases slightly from 2.72 to 6.351 nm with plasma treatment. Water contact angles do not typically exceed 120° on surfaces[24] without roughness. This likely explains the 112.3° water contact angle observed in the present study and indicates that chemical modification of the surface rather than changes in morphology underly the hydrophobic property of the HMDSO polymer coating.

3.6. LigaSure™ Force Measurements

The forces required to open the jaw of LigaSure™ Atlas instruments after tissue fusion is completed are plotted in Figure 8. Both the HMDSO polymer-coated and chromium nitride-coated instruments exhibit significantly less sticking than uncoated instruments through 100 sealing cycles. The HMDSO polymer-coated instrument is markedly less sticky than the chromium nitride-coated instrument up to 50 sealing cycles. The increase in sticking force of the HMDSO polymer-coated instrument after 50 sealing cycles may be due to film failure from the extreme conditions at the jaw during tissue fusion, however the overall result of 3.85 lbs for the HMDSO polymer coating compares favorably to the historical average of 5.6 lbs for the vacuum-

DOI: 10.1002/ppap.201100155

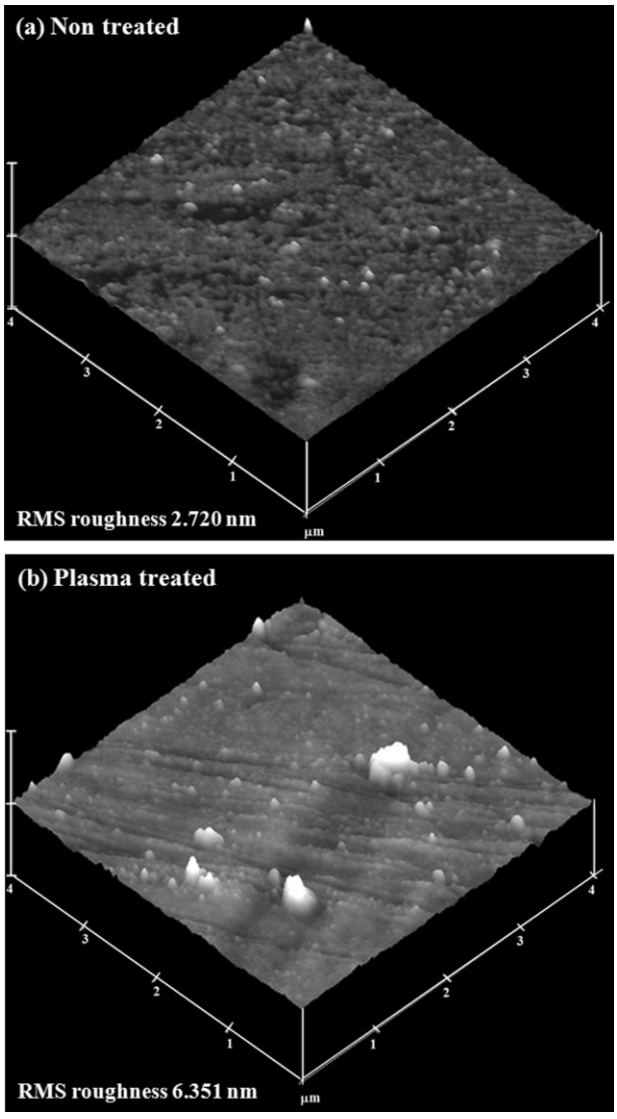

Figure 7. AFM images of (a) non-treated and (b) plasma-treated glass slides. Main argon flow is fixed at 800 sccm and deposition is carried out for 60 s at 25 W input power and 1.0% HMDSO.

deposited chromium-nitride coating developed previously at Covidien.

4. Conclusion

To reduce undesired tissue adhesion to energy-based surgical instruments, we developed a coaxial type atmospheric pressure plasma jet that operates at lower power and temperature compared to other sources in the literature,[25,26] but is effective for coating tissue fusion devices. Plasma is stably generated at 25 W input power with entrained HMDSO monomer concentration up to 2.0%. We find that the water contact angle increases (from 29.3 to

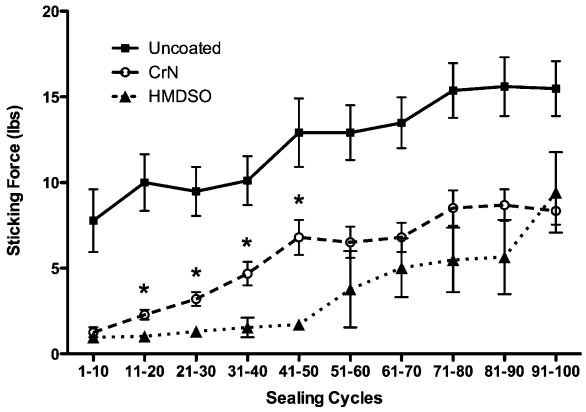

Figure 8. Measuring required opening force of LigaSure™ Atlas jaw electrodes following tissue fusion. Asterisk denotes significant difference ($p < 0.05$) between HMDSO polymer coatings by atmospheric plasma jet and vacuum-deposited chromium nitride (CrN) coatings.

112.3°) and the surface energy decreases (from 42 mN m^{-1} to less than 32 mN m^{-1}) with plasma treatment. AFM and FTIR data show that the hydrophobic functionality stems from the chemical structure of the deposited polymer rather than surface morphology. Finally, we have illustrated the practical advantages of the non-stick coating process for electrode jaws employed in LigaSure™ tissue fusion devices.

Acknowledgements: Research Work partially supported by NSF. The authors are grateful to Mr. N. C. Jung for assistance with AFM. This work was partially supported by Covidien and Colorado State University as well as Mid-career Researcher Program through NRF grant (2011-0015395) funded by the MEST and the Korea Ministry of Education, Science, and Technology through its Brain Korea 21 program.

Received: August 5, 2011; Revised: November 27, 2011; Accepted: December 13, 2011; DOI: 10.1002/ppap.201100155

Keywords: atmospheric pressure plasmas; hydrophobic coatings; plasma-enhanced chemical vapor deposition (PECVD); plasma polymerization

[1] S. J. Lee, B. G. Paik, G. B. Kim, Y. G. Jang, *Jpn. J. Appl. Phys.* **2006**, *45*, 2A.
[2] I. P. Parkin, R. G. Palgrave, *J. Mater. Chem.* **2005**, *15*, 1689.
[3] G. X. Shen, Y. C. Chen, L. Lin, C. J. Lin, D. Scantlebury, *Electrochim. Acta* **2005**, *50*, 5083.
[4] S. Sathiyanarayanna, S. S. Azim, G. Venkatachari, *Electrochim. Acta* **2007**, *52*, 2068.

[5] M. Ma, R. M. Hill, *Curr. Opin. Colloid Interface Sci.* **2006**, *11*, 193.
[6] P. K. Chu, J. Y. Chen, L. P. Wang, N. Huang, *Mater. Sci. Eng. R* **2002**, *36*, 143.
[7] H. E. Colley, G. Mishra, A. M. Scutt, S. L. McArthur, *Plasma Process. Polym.* **2009**, *6*, 831.
[8] L. Kleinen, I. Syring, N. Laube, *Plasma Process. Polym.* **2009**, *6*, 541.
[9] C. Huang, C. H. Pan, C. H. Liu, *Thin Solid Films* **2010**, *518*, 3570.
[10] D. Hegemann, H. Brunner, C. Oehr, *Plasma Polym.* **2002**, *6*, 221.
[11] S. H. Kim, J. H. Kim, B. K. Kang, H. S. Uhm, *Langmuir* **2005**, *21*, 12213.
[12] A. S. Aroca, M. M. Pradas, J. L. G. Ribelles, *Polymer* **2007**, *48*, 2071.
[13] J. H. Kim, G. Liu, S. H. Kim, *J. Mater. Chem.* **2006**, *16*, 977.
[14] C. Cheng, Z. Liye, R. J. Zhan, *Surf. Coat. Technol.* **2006**, *200*, 6659.
[15] K. Aumaille, C. Valle, A. Granier, A. Goullet, F. Gaboriau, G. Turban, *Thin Solid Films* **2000**, *359*, 188.
[16] D. S. Wavhal, J. Zhang, M. L. Steen, E. R. Fisher, *Plasma Process. Polym.* **2006**, *3*, 276.
[17] A. Bellel, S. Sahli, Z. Ziai, P. raynaud, Y. Segui, D. Escich, *Surf. Coat. Technol.* **2006**, *201*, 129.
[18] Y. Y. Ji, S. S. Kim, O.-Pil. Kwon, S. H. Lee, *Appl. Surf. Sci.* **2009**, *255*, 4575.
[19] J. S. Kim, R. H. Friend, F. Cacialli, *J. Appl. Phys.* **1999**, *86*, 6.
[20] A. Grill, *Annu. Rev. Mater. Res.* **2009**, *39*, 49.
[21] R. Morent, N. De Geyter, T. Jacobs, S. Van Vlierberghe, P. Dubruel, C. Leys, E. Schacht, *Plasma Process. Polym.* **2009**, *6*, S537.
[22] R. N. Wenzel, *Ind. Eng. Chem.* **1936**, *28*, 988.
[23] A. B. D. Cassie, S. Baxter, *Trans. Faraday Soc.* **1944**, *40*, 546.
[24] S. H. Wu, *Polymer Interface and Adhesion*, Marcel Dekker, New York, USA **1982**.
[25] M. Nagai, M. Hori, T. Goto, *J. Appl. Phys.* **2005**, *97*, 123304.
[26] A. Milella, R. D. Mundo, F. Palumbo, P. Favia, F. Fracassi, R. d'Agostino, *Plasma Process. Polym.* **2009**, *6*, 460.

DOI: 10.1002/ppap.201100155